# Blockchain Integrated Neural Networks: A New Frontier in MRI-based Brain Tumor Detection

Subrata Banik[1], Nani Gopal Barai[2], F M Javed Mehedi Shamrat[3]

Bangladesh Japan Information Technology Limited (BJIT Limited), Dhaka, Bangladesh[1, 2]

Department of Computer System and Technology, University of Malaya, Kuala Lumpur, Malaysia[3]

*Abstract*—Brain tumors originating from uncontrolled growth of abnormal cells in the brain, presents a significant challenge in healthcare due to their various symptoms and infrequency. While Magnetic Resonance Imaging (MRI) is essential for accurately identifying and diagnosing malignant tumors, manual interpretation is often complex and sensitive to mistakes. To address this, we introduce BrainTumorNet, a specialized convolutional neural network (CNN) created for MRI-based brain tumor diagnosis. We ensure improved image quality and a robust dataset for model training by including preprocessing approaches involving CLAHE and data augmentation. Additionally, we integrated a blockchain-based data retrieval technology to enhance the security, traceability, and collaboration in MRI data management across several medical institutions. This blockchain framework ensures that MRI data, once input from hospitals, stays immutable and can be safely retrieved based on unique hospital IDs, promoting a trustable environment for data exchange. Performance assessments conducted on multiple MRI datasets showcased BrainTumorNet's commendable proficiency, with accuracy rates of 98.66%, 97.17% and 94.24% on the dataset 1, dataset 2, and dataset 3, respectively. The model's performance was evaluated using a comprehensive set of metrics, including accuracy, specificity, recall, precision, f1-score, and confusion matrix. These measures are essential for evaluating a model's strengths and limits, emphasizing BrainTumorNet's ability to generate accurate and relevant predictions and its effectiveness in determining negative classification. BrainTumorNet's performance was compared with six renowned deep learning architectures: VGG16, ResNet50, AlexNet, MobileNetV2, InceptionV3, and DenseNet121. Our work highlights BrainTumorNet's potential capabilities in simplifying and boosting the accuracy of MRI-based brain tumor diagnosis while ensuring data integrity and collaboration through blockchain.

*Keywords—Brain tumor; MRI imaging; BrainTumorNet; deep learning; image classification; augmentation*

## I. INTRODUCTION

Brain tumors develop from abnormal cell growth in the brain [1]. While cells normally follow a regular development and death cycle, sometimes they expand uncontrolled, resulting to harm in the brain. There are around 120 distinct forms of brain tumors and central nervous system (CNS) exist. In 2021, the American Cancer Society anticipated that brain and CNS cancers will cause 18,600 adult and 3,460 child deaths. The probability of surviving five years after being diagnosed is roughly 36%, and 10 years is 31% [2]. In 2019, the National Cancer Institute recorded 86,010 new cases of brain and CNS cancers in the U.S. It's believed that roughly 700,000 Americans live with a brain tumor, with 60,800 of them being non-malignant and 26,170 being cancerous [3]. Globally, the World Health Organization recorded roughly 9.6 million new cancer diagnoses in 2018 [4].

Early diagnosis of brain tumors is vital for patient survival. Analyzing brain tumor images effectively is vital to determining a patient's health state. Physicians and radiologists traditionally scan magnetic resonance (MR) images to discover abnormalities. However, this strategy depends greatly on the medical skill of the practitioner [5]. Differences in experience and the complexity of the imagery may make diagnosis with the human eye challenging. Doctors may struggle to rapidly analyze MR images because they often include several abnormalities or unnecessary data. The difficulty of accessing this large quantity of information increases as the number of data increases, making manual tumor identification time-consuming and costly. There's a rising demand for an autonomous computer-aided diagnostics (CAD) system to solve these issues. Such technologies may help doctors and radiologists by enabling fast and precise identification of cancers, thereby contributing to preserving human lives.

Artificial intelligence (AI) provides automation with capacities following human brain functions, such as learning and problem-solving. In the field of brain tumor identification and diagnosis, AI's accuracy provides crucial help, particularly considering the sensitive nature of the task. There are several initiatives to improve brain tumor categorization. However, the variation in tumor properties, such as their form, texture, and contrast variations across people, continues to be a problem. Machine learning (ML) and deep learning (DL), two branches of AI, have brought in a new era for the practice of neurosurgery. These cutting-edge methods include data preparation, feature extraction, selection, reduction, and classification as their final steps. Recent research [6] reveals that AI permits neurosurgeons to perform surgeries with unsurpassed confidence, enabling more precise brain tumor diagnosis.

Deep learning (DL) is an advanced version of machine learning that dives into data using multi-layered representations. By establishing a feature hierarchy, DL ensures fundamental features aid in developing advanced ones. This technique strengthens classic neural networks by incorporating several hidden layers between input and output, allowing them to capture complicated, non-linear relationships. Because of its excellent performance in recent years, DL has become the frontrunner in many medical image analysis difficulties, including tasks like image denoising, segmentation, authentication, and classification.

Brain tumors, due to their various appearances and sporadic frequency, have long been a main topic of worry in the medical community. Though useful, traditional diagnostic approaches often depend on human mistakes, particularly given the delicate nuances of MRI imaging. Recognizing these problems, we designed BrainTumorNet. Designed to overcome current diagnostic inadequacies, BrainTumorNet employs the ability of deep learning to negotiate the difficulties of MRI-based tumor identification. Our objectives for BrainTumorNet are not simply confined to enhanced diagnostic capabilities; we also emphasize a smooth, transparent, and most crucially, a secure data flow. This is where the integration of blockchain technology plays a key role, bringing in an approach where data integrity and trustworthiness become the standard rather than the exception. As our study develops a comprehensive strategy, blending cutting-edge AI with the resilience of blockchain, we intend to redefine the standards in brain tumor detection. The key findings of this research are:

- BrainTumorNet, a novel proposed model, demonstrated significant proficiency in identifying brain tumors using multiple MRI datasets.

- The addition of the CLAHE preprocessing approach significantly improved the image quality, leading to better model performance.

- Utilized a rigorous data augmentation method to increase the dataset's size and prevent the model from overfitting and improve its generalizability across various MRI images.

- We implemented a blockchain-based system for MRI data retrieval in recognition of the essential requirement for data security and traceability in medical diagnostics. This integration promises a clear, dependable, and immutable data handling procedure.

- Using six thorough performance indicators on three different datasets, we systematically evaluated BrainTumorNet's effectiveness. This comprehensive assessment confirmed the model's consistently good performance, proving its durability and dependability.

## II. LITERATURE REVIEW

CNN has been extensively employed to address various issues, but its performance in health-related image processing applications is outstanding. Several techniques have been developed based on DL to identify brain tumors on MRI images in recent years. Most of them focused on binary segmentation to identify brain tumors.

Zhao et al. [7] developed an inventive method for brain tumor segmentation by integrating a complete Convolutional Neural Network (CNN) with Conditional Random Fields (CRFs). This unified framework assured visual excellence and spatial coherence in the segmentation outcomes. They employed three segmentation models trained on 2D image segments and slices from axial, coronal, and sagittal views. These models were combined using a voting-based fusion approach for precise tumor segmentation. On the other hand, Mohsen et al. [8] utilized a Deep Neural Network (DNN) classifier to differentiate an MRI dataset into four categories: normal tissue, glioblastoma, sarcoma, and metastatic bronchogenic carcinoma tumors. They incorporated Principal Component Analysis (PCA), an effective feature extraction technique, with the discrete wavelet transform (DWT) before classification. The ensuing evaluations showcased remarkable performance across all metrics.

Paul et al. [9] focused on 989 axial images, intending to simplify the neural network procedure by omitting the incorporation of three distinct axes with redundant diagnostic information. Both fully connected networks and CNNs were utilized for classification. When trained with axial data, the neural network achieved an impressive accuracy of 91.43% employing five-fold cross-validation, indicating its classification precision. On the other hand, Ari et al. [10] presented a three-step method. The initial phase contained preprocessing, where nonlocal means and local smoothing techniques decreased noise. In the subsequent step, the extreme learning machine with local receptive fields (ELM-LRF) was employed to classify cranial MR images as benign or malignant. Finally, image processing techniques segmented tumor areas in the third phase.

In this research, Abiwinanda et al. [11] aimed to train a CNN model to identify the three most prevalent forms of brain malignancies: gliomas, meningiomas, and pituitary tumors. They developed the simplest conceivable CNN architecture, consisting of one layer each of convolution, max-pooling, and flattening, followed by a complete connection from a single hidden layer. Using the basic architecture and no previous region-based segmentation, the study attains a maximum validation accuracy of 84.19%. Afshar et al. [12] have recently included newly generated CapsNets to alleviate the problem with CNNs that fail to properly exploit spatial interactions. Since the relationship between the tumor and the neighboring tissue is a crucial sign of tumor kind. Because of this, a specialized version of the CapsNet architecture for classifying brain tumors is proposed, including the tumor's coarse borders as additional inputs inside its pipeline to sharpen its attention.

However, Khan et al. [13] proposed a method comprising three critical phases: preprocessing, brain tumor segmentation applying k-means clustering, and benign/malignant tumor identification via a fine-tuned VGG19 model. This method has been assessed employing the BraTS 2015 benchmark dataset. Furthermore, they proposed synthetic data augmentation to expand the training dataset size, which consequently enhanced the classification accuracy. Yahyaoui et al. [14] offer a new semantic approach by fusing 2D and 3D MRI data in this study. Preprocessing, categorization, and fusion are the three stages that make up the whole system. To classify 2D brain data, the DenseNet model is used, and the 3D-CNN model was created specifically for 3D brain scans. Authors relied on a domain-specific ontology to accomplish the fusion of the output classes.

Furthermore, Murthy et al. [15] deployed the Optimized Convolutional Neural Network with Ensemble Classification (OCNN-EC) for tumor image classification. This deep learning approach encompasses an ensemble classifier containing a Deep Neural Network (DNN), an autoencoder, and a Support

Vector Machine (SVM). This ensemble replaces the completely connected layer once the ACV-DHOA has optimized the count of convolutional layers and hidden neurons. In this study, Latif et al. [16] argue that features from the MR images are extracted using a deep CNN network and then input into a support vector machine classifier. This research uses the BraTS dataset to categorize Gliomas into many classes. The suggested method attained a remarkable 96.19% accuracy.

Several recognized limitations in MRI-based brain tumor diagnosis were clear in light of available studies. Notably, many existing models struggle with accuracy problems, the difficulties of adding data to MRI datasets, and the complexity of managing various MRI data sources. We established

BrainTumorNet to close these gaps and improve the diagnostic capability. The purpose of our proposed model is to achieve higher performance in the detection of brain tumors from MRI images. BrainTumorNet aims to establish a new standard in both accuracy and reliability in the field of brain tumor diagnosis, further enhanced by blockchain technology for secure and transparent data administration.

## III. METHODOLOGY

This section highlights the main methods we employed during our research, including image preprocessing, deep feature extraction, blockchain integrity, and deep learning algorithms. The process of tumor detection is presented in Fig. 1.
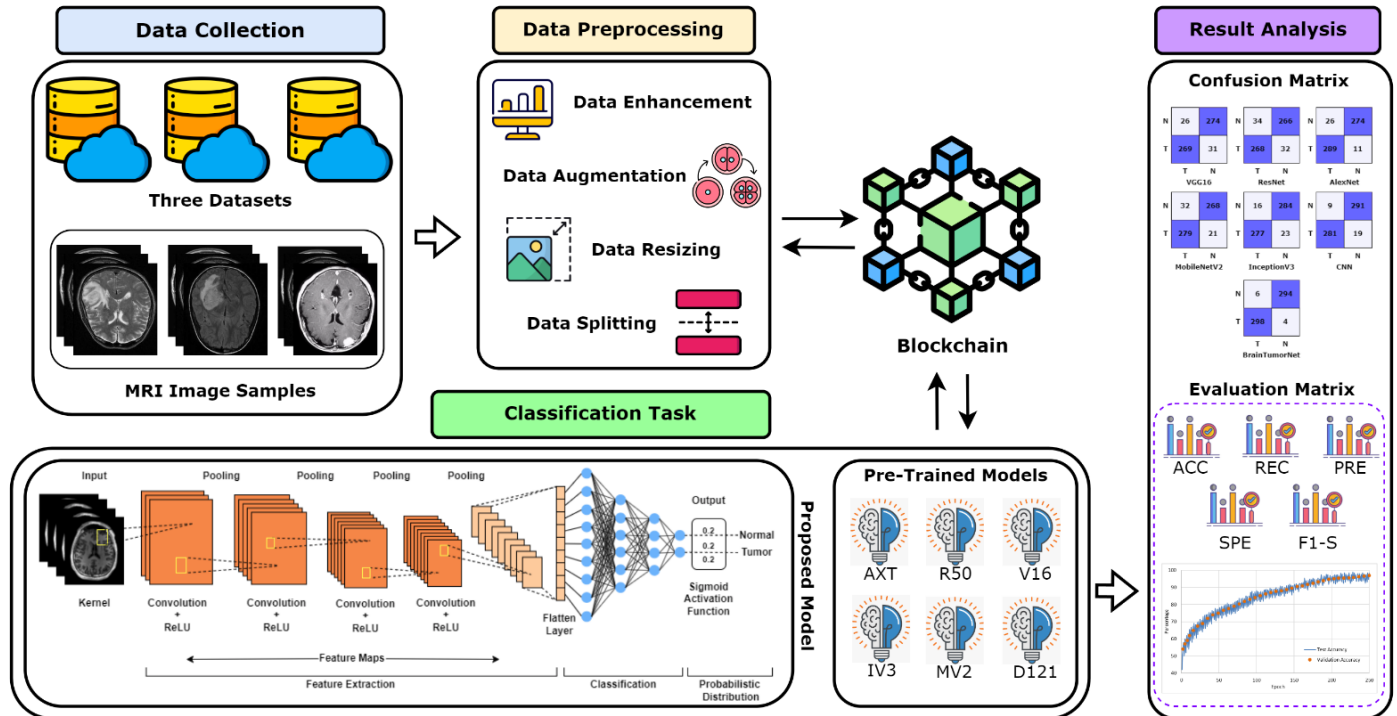


Fig. 1. The entire system of the proposed model BrainTumorNet.

### A. Data Collection:

For the study, three publicly available datasets are used. The datasets are image datasets that contain MRI images of the brain. The detailed description of the employed dataset is stated below:

*1) Dataset 1 (DT1):* Br35H: Brain Tumor Detection 2020 [17] is the first dataset used in the study. It is an MRI image dataset. The dataset consists of 1500 images positive for brain tumors and 1500 images of normal brains. The normal and tumor class dataset samples are shown in Fig. 2(a).

*2) Dataset 2 (DT2):* The BraTS 2019 [18] is the second dataset used in this study. The dataset contains 1500 MRI images of the brain with tumor and 1500 MRI images of the normal brain. The sample images of this dataset are presented in Fig. 2(b).
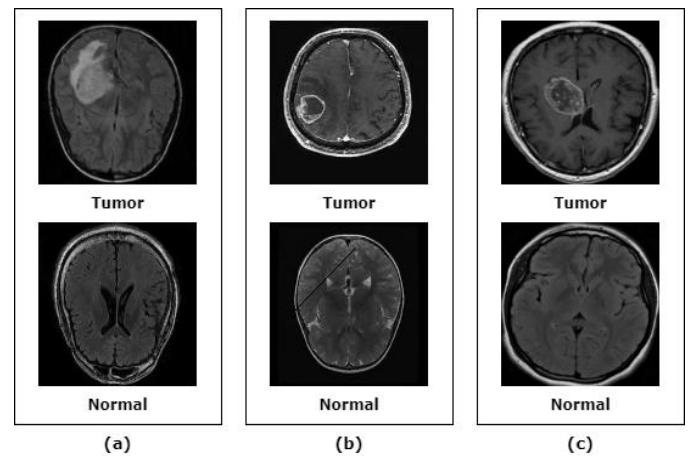


Fig. 2. Data sample of the three datasets (a) DT1 (b) DT2 (c) DT3.

*3) Dataset 3 (DT3):* The third dataset used in the study is available in the Kaggle data repository [19]. This is an unbalanced image dataset. It contains 170 MRI images of normal brain and 230 images of brain with tumor. The sample images of the normal and tumor class of DT3 are presented in Fig. 2(c).

### B. Data-preprocessing:

*1) Clache:* Contrast limited adoptive histogram equalization (CLAHE) is used to enrich the image quality. CLAHE improves the contrast of the MRI image. Images are normalized using this technique, which also highlights finer information for Machine Learning (ML) classifiers to pick up on. By boosting contrast locally, the CLAHE method gets beyond the limitations of traditional, global approaches. Critical hyper-parameters for this technique are the tile size and clip limit. Multiple permutations of all these settings are examined before the ideal values of tileGridSize (8, 8), and the clip limit is settled on (3.7). Algorithm 1 displays the process of CLAHE.

---

**Algorithm 1:** CLAHE Working Process

---

**Procedure** CLAHE (Image $I$, ClipLimit c, GridSize g)

$I_{gray} \leftarrow$ Convert $I$ to grayscale

$CLAHE_{object} \leftarrow$ Initialize CLAHE with c and g

$I_{processed} \leftarrow$ Apply $CLAHE_{object}$ on $I_{gray}$

Save $I_{processed}$ as 'clahe_output.jpg'

**Return** $I_{processed}$

**End**

---

*2) Data augmentation:* The datasets, DT1 and DT2 are well balanced datasets. However, DT3 is a highly imbalanced dataset and consists of a small amount of data. Since ML models require a fairly large dataset to train and produce efficient performance result. To do this, we leverage the ImageDataGenerator class in the Keras library to generate high-quality images for the expansion of our training data. Table I has the image-making parameters. After augmentation, the final count of the DT3 is 500 images of normal brain and 500 images of brain tumor. Algorithm 2 represents the procedure of augmentation.

TABLE I.        ATTRIBUTES OF IMAGEDATAGENERATOR

| Attributes | Values |
|---|---|
| Shear_range | 0.3 |
| Zoom_range | 0.2 |
| Vertical flip | True |
| Horizontal flip | True |
| Rescale | 1/255 |

---

**Algorithm 2:** Augmentation for Balancing Image

---

**Procedure** AugmentData

Define ImageDataGenerator attributes

Function LOAD_IMAGES (directory)

**Return** images from *directory*

End

*NormalImages* ← LOAD_IMAGES (normal_dir)

*TumorImages* ← LOAD_IMAGES (tumor_dir)

**While** count of normal_images ! 500 **do**

Augment 'normal' images

End

**While** count of tumor_images ! 500 **do**

Augment 'tumor' images

End

Return Count

End

---

*3) Resize image:* For uniformity's sake, we resize every picture in the collection to 128×128 pixel, since the original dimensions of images in the three datasets (DT1, DT2, and DT3) vary substantially.

*4) Dataset splitting:* The datasets are divided into training and validation subsets. The division is done at a ratio of 80:20, where 80% of each data belongs to the training set and the remaining 20% to the test set. Table II shows the data division of each set.

TABLE II.        DATA DISTRIBUTION OF THE DATASETS

| Dataset | Training set | Test set | Total |
|---|---|---|---|
| DT1 | 2400 | 600 | 3000 |
| DT2 | 2400 | 600 | 3000 |
| DT3 | 800 | 200 | 1000 |

### C. Blockchain Framework for Secure Data Management in BrainNet

Our proposed system incorporates blockchain architecture to ensure effective and secure data retrieval and sharing procedure designed for managing medical MRI data. Many institutions may cooperatively exchange and store MRI information to improve the BrainTumorNet model's detection abilities without compromising patient data integrity. Our work emphasizes the MRI data retrieval and sharing procedures inside our method, based upon the multi-organization blockchain designs mentioned by [20], [21].

*1) Blockchain-based MRI data retrieval process:* In the framework of our study, every participating data source/hospital provides MRI data, storing it as a unique transaction inside the blockchain network. Before this data is placed into the blockchain, it undergoes a preprocessing stage. Initially, the MRI images are improved using the CLAHE approach, which increases the contrast and overall visibility of tumor locations in the images. Following this, Data Augmentation methods are applied to extend the dataset intentionally. This assures increased variety and assists in training the BrainTumorNet model more robustly.

Retrieving this data from the blockchain nodes hinges on two key parameters: the distance between the nodes ($d$) and the unique ID of the hospital ($ID$). Each hospital denoted as $x_i$, is assigned a unique ID, determined in part by its distance $d_{ij}$ from another hospital $x_j$. This can be represented as,

$$ID_i = f(x_i, d_{ij}) \qquad (1)$$

where, $f$ is a function computing the ID based on the hospital's attributes and its distance from other hospitals.

The blockchain system maintains log tables that register these unique IDs, ensuring that data integrity is maintained at all times. When BrainTumorNet needs to access specific MRI datasets for its diagnostic tasks, it retrieves the relevant data from the corresponding hospitals using the retrieval function $R(ID_i)$. This function returns the data $x_i$ if $ID_i$ exists in the log table, otherwise it returns to error.

Moreover, the neighborhood distance between two sources, $x_i$ and $x_j$, plays a critical role in efficient data access. The distance $d_{ij}$, can be determined by,

$$d_{ij} = g(l(x_i), l(x_j)) \qquad (2)$$

where, $g$ is the distance function and $l(x)$ represents the location of source $x$.

This research effort aims to establish a new benchmark in secure, transparent, and collaborative medical diagnostics, laying the foundation for further advancements in this interdisciplinary field by combining the robustness of blockchain technology with the diagnostic prowess of BrainTumorNet and rigorous preprocessing steps.

### D. Deep Learning Models for Classification

Our proposed model's major objective is to automatically identify people who have brain tumors while decreasing classification time and increasing accuracy. For the purpose of finding brain tumors utilizing multiples MRI datasets, we proposed a novel, reliable and robust CNN model BrainTumorNet. To establish the most effective transfer learning strategy for the classification assignment, six pre-trained models including VGG16, ResNet50, AlexNet, MobileNetV2, InceptionV3, and DenseNet121 are tested. The significant characteristics and some essential properties of the selected deep CNN models are compiled in Table III The next section includes an entire discussion of the model utilized in this study.

*1) AlexNet:* This model is consisting of five convolution layers and three fully linked layers. certain number of convolution layers are succeeded by the max-pooling layer (1, 2, and 5 layers). The ReLU nonlinearity is applied to the output of every fully connected and convolutional layer. Each of the connected layers has 4096 neurons [22]. During training, neurons are "turned off" with a predefined probability to prevent data over-adjustment using a regularization technique known as dropout [23].

TABLE III. PROPERTIES OF THE DEEP LEARNING MODELS EMPLOYED IN THIS RESEARCH

| Model | Input Shape | Custom Input Shape | Parameters | Size (MB) |
|---|---|---|---|---|
| VGG16 | 224×224 | 224×224 | $138 \times 10^6$ | 552 |
| ResNet50 | 224×224 | 224×224 | $25.6 \times 10^6$ | 102 |
| AlexNet | 227×227 | 224×224 | $60 \times 10^6$ | 240 |
| MobileNetV2 | 224×224 | 224×224 | $3.5 \times 10^6$ | 14 |
| InceptionV3 | 229×229 | 224×224 | $23.8 \times 10^6$ | 95 |
| DenseNet121 | 224×224 | 224×224 | $8 \times 10^6$ | 32 |
| BrainTumorNet | 222×222 | - | $2.16 \times 10^6$ | 10 |

*2) ResNet50:* ResNet50 [24] is a 50-layer Convolutional Neural Network (CNN) composed of 48 fully connected layers, one max pooling layer, and one average pooling layer. It's capable of performing up to $3.8 \times 10^9$ floating-point computations. To resolve the vanishing gradient issue prevalent in traditional CNNs and expedite the training process, ResNet50 employs a spectrum of convolutional filters of varying sizes [25]. With fewer filters, ResNet's operates more promptly. This architecture is trained using approximately 23 million parameters. The network is designed to receive images where the height, breadth, and channel dimensions are multiples of 32.

*3) VGG16:* The Visual Geometric Group is referred to as VGG [26]. Simonay and Zimmerman [27] created the VGG model. VGG employs 3×3 convolutional layers that are layered on top of one another and become deeper over time. Max pooling layer is responsible for reducing the volume size. Afterwards, a softmax classifier is followed by two completely connected layers with a total of 4096 nodes each [27].

*4) InceptionV3:* At the ImageNet Recognition Challenge, Google introduced Inception version 3 [28]. The Auxillary Classifiers contain a label smoothing classifier, a factorized 7×7 convolution classifier, a batch norm classifier, an RMSProp optimizer, and a downscaling classifier for extracting and augmenting data from label sequences. The InceptionV3 model's training time is shortened by substituting bigger convolutions for smaller ones. Several optimization methods may be used to remove constraints and make an InceptionV3 model more flexible. The model is designed employing max pooling, convolutions, concatenations, dropouts, and fully-connected layers.

*5) MobileNetV2:* MobileNetV2 [38] is built upon an inverted residual structure, with residual connections

interconnecting its bottleneck layers. The intermediate expansion layer utilizes lightweight depth-wise convolutions to provide non-linear feature filtering. Following the initial convolutional layer with 32 filters, MobileNetV2 incorporates 19 residual bottleneck layers, resulting in a total of 53 layers for the network. The model has been pre-trained using over a million images from the ImageNet database, classified into 100 distinct categories. As a result, the network has gathered an enormous number of features from a diverse multitude of images.

*6) DenseNet121:* The Dense Convolution Network is a deep learning model that employs feedforward to link each layer to all subsequent layers [29]. DenseNet has (L(L+1))/2 direct lines compared to L connections for conventional L-layer CNNs. A feature map may be found in every layer of the model. Each layer's feature map serves as the following layer's input. It allows for the most information to be sent throughout the network by linking all levels directly to one another. DenseNet's primary benefits are a large reduction in parameter count, prevention of gradient runaway, improvement of feature diffusion, and encouragement of feature reuse. DenseNet needs fewer parameters than conventional CNN since the feature map is not repeatedly trained. Additionally, DenseNet uses regularization to lessen the possibility of overfitting. Each of the four dense blocks in DenseNet121 has six, twelve, twenty-four, and sixteen convolution blocks.

*7) BrainTumorNet (Proposed Model):* BrainTumorNet model is both small in size and computationally effective, improving performance across various datasets. This model is precisely designed for CNN that processes grayscale images with dimensions of 222×222×1 to identify brain tumors from MRI scans. The network is designed with four distinct blocks that have been optimized for feature extraction. Each of these blocks begins with a Conv2D layer, which is statistically stated by,

$$I'_{x,y,k} = \sum_{i=-\infty}^{\infty} \sum_{j=-\infty}^{\infty} I_{x-i,y-j,k} \cdot K_{i,j,k} \qquad (3)$$

where, $I_{x,y,k}$ is the input feature map at position $(x, y)$ for the kth channel. $K_{i,j,k}$ represents the kernel or filter at position $(i, j)$ for the kth channel and $I'_{x,y,k}$ is the output of feature map after convolution at position $(x, y)$ for the kth channel.

Following the convolutional transformation, there is a MaxPooling layer, which is presented as,

$$P_{x,y,k} = max_{i=0}^{s-1} \; max_{j=0}^{s-1} \; I_{sx+i,sy+j,k} \qquad (4)$$

Here, $P_{x,y,k}$ is the pooled output at position $(x, y)$ for the kth channel, and $s$ denotes the pooling window size.

Each block ends with a batch normalization layer, stabilizing the activations and ensuring the features remain standardized. As the depth of the network increases, the spatial dimensions are progressively reduced, encapsulating more complex and sensitive patterns essential to tumor identification. Once the entire spatial panorama has been thoroughly evaluated, the extracted features are flattened into a 1D tensor, covering a size of 10816. This tensor then runs across two dense layers, described by,

$$y = Wx + b \qquad (5)$$

Here, $y$ is the output of the dense layer, $W$ symbolizes the weight matrix, $x$ represents the input to the dense layer, and $b$ is the bias term.

The end of BrainTumorNet's activities is encapsulated in its last output layer, which is equipped with a sigmoid activation function. This design option provides binary classification capabilities, properly denoting whether the input MRI shows the existence or absence of a tumor. Table IV demonstrates the architecture of the proposed model BrainTumorNet. Fig. 3 illustrates a visual output of the proposed model.

This proposed model for detecting brain tumors using MRI images surpasses prior approaches through feature extraction and processing efficiency improvements. Increasing filters on convolutional layers are utilized to identify detailed features, which are essential for identifying brain tumor characteristics. Convolutional layers employ a balanced layout of 1×1 stride and 3×3 kernel size to optimize image processing, followed by max pooling. This arrangement minimizes the loss of information while preserving computational efficiency. Integrating BatchNormalization enhances learning stability, facilitating fast and consistent training. The model reaches the highest point with a binary classification output layer that is designed to ensure precise tumor detection. This architectural design signifies an important improvement in the accurate detection of brain tumors by addressing the distinct difficulties associated with MRI image analysis.
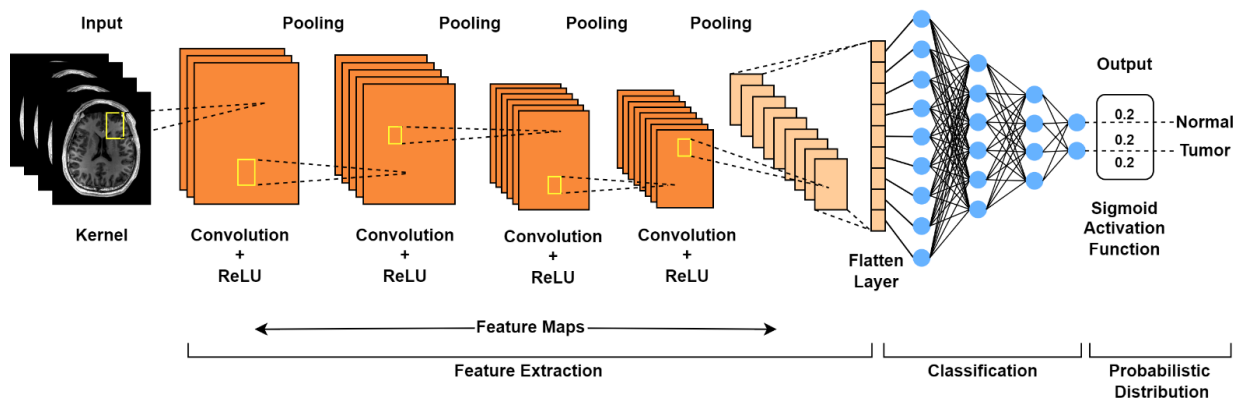


Fig. 3. The architecture of the proposed model BrainTumorNet.

TABLE IV.    DESCRIPTION OF BRAINTUMORNET ARCHITECTURE LAYERS USED FOR BRAIN TUMOR DETECTION

| Operation | Layer Name | No. of Filters | Stride Size | Kernel Size | Padding Size | No. of Channels | Input Shape | Output Shape |
|---|---|---|---|---|---|---|---|---|
| Input Image | Input Layer | - | - | - | - | 3 | $222 \times 222 \times 1$ | - |
| Convolution | Convolution 2D | 32 | 1×1 | 3×3 | Same | 32 | $222 \times 222 \times 1$ | $222 \times 222 \times 32$ |
| Pooling | Maxpooling | - | 2×2 | 2×2 | Valid | 32 | $222 \times 222 \times 32$ | $111 \times 111 \times 32$ |
| Normalization | BatchNormalization | - | - | - | - | 32 | $111 \times 111 \times 32$ | $111 \times 111 \times 32$ |
| Convolution | Convolution 2D | 32 | 1×1 | 3×3 | Same | 32 | $111 \times 111 \times 32$ | $111 \times 111 \times 32$ |
| Pooling | Maxpooling | - | 2×2 | 2×2 | Valid | 32 | $111 \times 111 \times 32$ | $55 \times 55 \times 32$ |
| Normalization | BatchNormalization | - | - | - | - | 32 | $55 \times 55 \times 32$ | $55 \times 55 \times 32$ |
| Convolution | Convolution 2D | 64 | 1×1 | 3×3 | Same | 64 | $55 \times 55 \times 32$ | $55 \times 55 \times 64$ |
| Pooling | Maxpooling | - | 2×2 | 2×2 | Valid | 64 | $55 \times 55 \times 64$ | $27 \times 27 \times 64$ |
| Normalization | BatchNormalization | - | - | - | - | 64 | $27 \times 27 \times 64$ | $27 \times 27 \times 64$ |
| Convolution | Convolution 2D | 64 | 1×1 | 3×3 | Same | 64 | $27 \times 27 \times 64$ | $27 \times 27 \times 64$ |
| Pooling | Maxpooling | - | 2×2 | 2×2 | Valid | 64 | $27 \times 27 \times 64$ | $13 \times 13 \times 64$ |
| Normalization | BatchNormalization | - | - | - | - | 64 | $13 \times 13 \times 64$ | $13 \times 13 \times 64$ |
| Flattening | Flatten | - | - | - | - | - | $13 \times 13 \times 64$ | 10816 |
| Fully Connected | Dense | 128 | - | - | - | - | 10816 | 128 |
| Fully Connected | Dense | 64 | - | - | - | - | 128 | 64 |
| Output | Dense | 2 | - | - | - | - | 64 | 2 |

### E. Hyperparameters Tuning:

The principal objective of this research is to develop the most efficient model BrainTumorNet for classifying brain MRI data. Hyperparameters are a group of factors that have the ability to impact the model's training process and provide the best outcomes [30-32]. These parameters include the volume of epochs, batch size, image size, optimizers, activation function, learning rate, decay rate, dropout rate and regularizer. During the experiment, we conducted several trials before settling on batch size, learning rate, regularization factor, etc. Different pre-trained models, including VGG16, ResNet50, AlexNet, MobileNetV2, InceptionV3, and DenseNet121, are used to execute the proposed brain tumor detection. Using a variety of optimizers, each model was assessed for 250 epochs. Each model is first tuned using Keras-tune to obtain the appropriate hyperparameter ranges. We employ the widely utilized grid search strategy for parameter tuning. Table V displays the parameters after tuning used during model training.

### F. Evaluation Matrix

Accuracy, Specificity, Recall, Precision, and F1-score are some of the performance metrics calculated to assess the models' efficacy. Accuracy measures the rate of a model produce accurate predictions. The relevant predictions of positive classes are determined by calculating precision.

Efficiency in predicting the negative class from the whole set of classes is measured by specificity. Contrarily, recall is the proportion of true positive classes that were anticipated. The F1-score measures how well specificity and recall are combined. Eq. (6) through Eq. (10) below express the parameters.

$$Accuracy = \frac{TP+TN}{TP+FP+TN+FN} \tag{6}$$

$$Precision = \frac{TP}{TP+FP} \tag{7}$$

$$Recall = \frac{TP}{TP+FN} \tag{8}$$

$$Specificty = \frac{TN}{TN+FP} \tag{9}$$

$$F1-score = 2 \times \frac{Precision \times Recall}{Precision+Recall} \tag{10}$$

Here, True Positive (TP) is the proportion of positive predictions that turned out to be accurate. True Negative (TN) is the accurately anticipated negative images. False Negative (FN) represents the count of positive photos that were incorrectly labeled as negative. Similarly, False Positive (FP) represents the count of negative data that were incorrectly labeled as positive.

TABLE V.    THE FINAL HYPERPARAMETERS USED TO TRAIN THE MODELS

| Model | No. of Epochs | Batch Size | Image Size | Optimizers | Activation Function | Learning Rate | Decay Rate | Dropout Rate | Regularizer |
|---|---|---|---|---|---|---|---|---|---|
| VGG16 | 250 | 64 | 224×224 | Adam | Softmax | 0.000001 | 1e-3 | 0.2 | 1e-4 |
| ResNet50 | 250 | 64 | 224×224 | SGD | ReLU | 0.0001 | 1e-4 | 0.2 | 1e-4 |
| AlexNet | 250 | 64 | 224×224 | Adagrad | ReLU | 0.00001 | 1e-2 | 0.2 | 1e-4 |
| MobileNetV2 | 250 | 64 | 224×224 | SGD | Softmax | 0.1 | 1e-4 | 0.2 | 1e-4 |
| InceptionV3 | 250 | 64 | 224×224 | Adam | Sigmoid | 0.001 | 1e-3 | 0.2 | 1e-4 |
| DenseNet121 | 250 | 64 | 224×224 | Adam | ReLU | 0.0000001 | 1e-2 | 0.2 | 1e-4 |
| BrainTumorNet | 250 | 128 | 222×222 | RMSProp | Sigmoid | 0.01 | 1e-5 | 0.2 | 1e-4 |

## IV. EXPERIMENTAL RESULTS

### A. Experimental Setup

We utilized the Keras 2.10.0, TensorFlow 2.0, and Python 3.7 programming languages to execute the proposed models and produce results. Visualization was done using the Seaborn and Matplotlib packages. System specifications include AMD Ryzen 7 running at 3.90 GHz, 32 GB of RAM, a MD Radeon RX 580 series GPU, and a Windows 10 setup.

### B. Result Analysis

Six different transfer learning models and novel BrainTumorNet model were employed in the study to detect brain tumor from MRI data. Furthermore, the seven models are employed on the three datasets containing MRI images of the brain. The purpose of the study is to identify a robust model that can classify MRI data to diagnose brain tumor. The models were run for 250 epoch and the outcome of each epoch are recorded for all three datasets. Using Eq. (6) through Eq. (10), we can calculate the performance parameters of each model and so assess how well each model performs.

In Fig. 4 we can see the results of the performance indicators for DT1. Among the transfer learning models, it is seen, the model CNN consistently displays high performance, with an accuracy of 95.34%. A precision of 96.14% was attained, along with 95.78% recall, 96.32% specificity, and 95.95% f1-score. It is followed by InceptionV3 with specificity of 92.55%, similarly the model falls well short of perfection in accuracy (93.5%), precision (92.17%), recall (95.78%) and f1-score (93.13%). Likewise, the other models, including VGG16, AlexNet, MobileNetV2, and ResNet50, all have subpar accuracy (90.47%, 93.75%, 91.24% and 89.02%, respectively). Contrary to the transfer learning models, the proposed model performs with exceptionally high measures. The accuracy of the proposed model BrainTumorNet is 98.66%. Similarly, the specificity is 98.59% and the f1-score is 97.69%.

Fig. 5 displays the outcomes of DT2's key performance metrics. The CNN model shows the highest classification efficiency among the transfer learning models with an accuracy of 94.76% and an f1-score of 94.98%. The accuracy score of VGG16, ResNet50, AlexNet, MobileNetV2 and InceptionV3 are 85.78%, 91.45%, 92.01%, 89.71% and 90.83% respectively. Performance-wise, the proposed BrainTumorNet model is much superior to transfer learning methods with an accuracy of 97.17%.

The results of DT3 are recorded and presented in Fig. 6. Similar to the other datasets, the CNN model has the best classification efficiency among the transfer learning models in DT3 with an accuracy of 92.5% and an f1-score of 92.79%. Similar to the previous datasets, in DT3, the BrainTumorNet shows the highest efficiency. The classification accuracy of the model is 94.24%. The precision, recall, specificity, and f1scores are 96.34%, 95.06%, 94.59%, and 95.69%, respectively.

The performance matrix shows that the proposed fine-tuned model performs consistently with the highest accuracy over the three datasets. However, the classification accuracy of the three datasets varies. The datasets DT1 and DT2 achieve accuracy of 98.66% and 97.17%, respectively. These accuracies are quite similar to the accuracy achieved from DT3, which is 94.24%.

The datasets DT1 and DT2 have higher counts of data compared to DT3. When employed on DT3, the models have less data to train on, so their performance suffers. On the contrary, when the BrainTumorNet model is trained and validated on DT1, it achieves the highest performance efficiency.
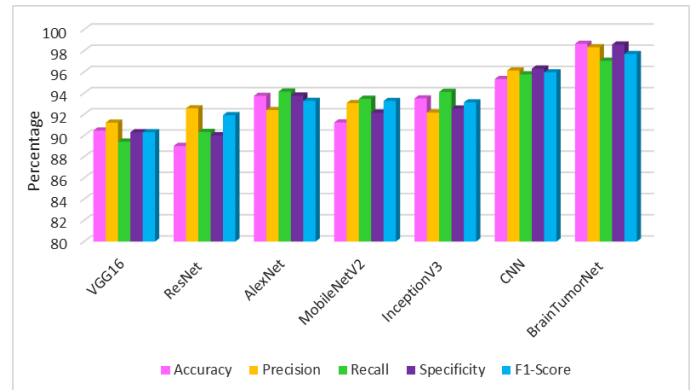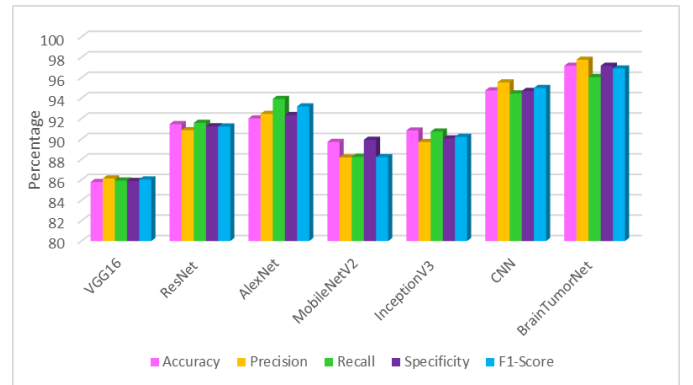


Fig. 4. Perfromance of the models for DT1.


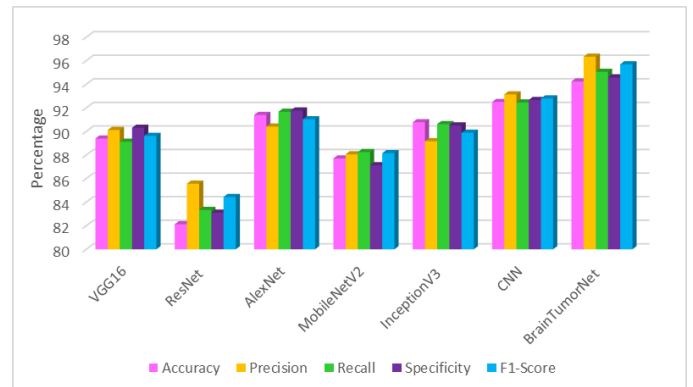
Fig. 5. Performance of the models for DT2.
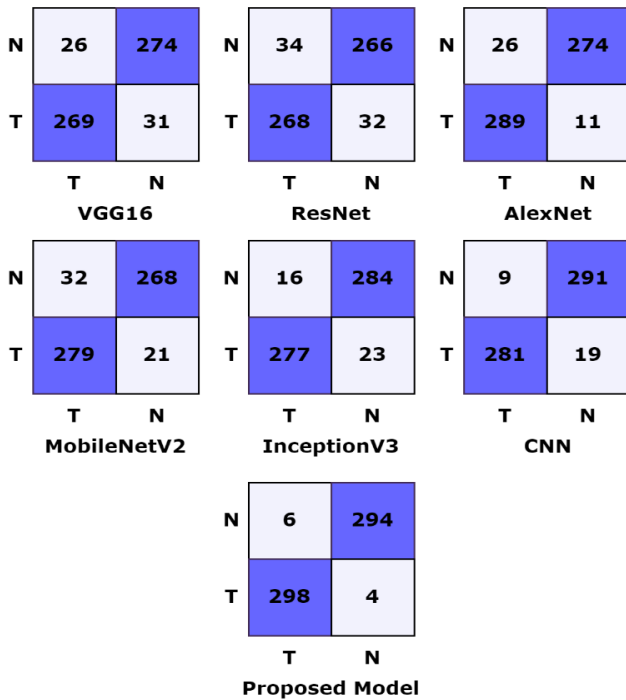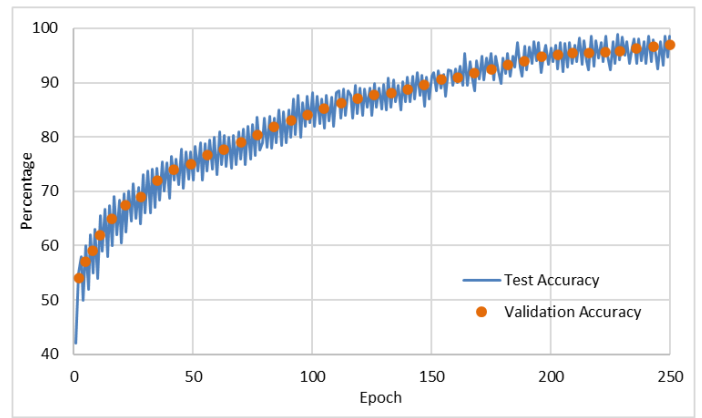


Fig. 6. Perfromance of the models for DT3.

Fig. 7.   Confusion Matrix of DT1 for the employed models.



(a)



(b)

Fig. 8.   (a) Accuracy and (b) Loss of proposed model on DT1 per epoch.
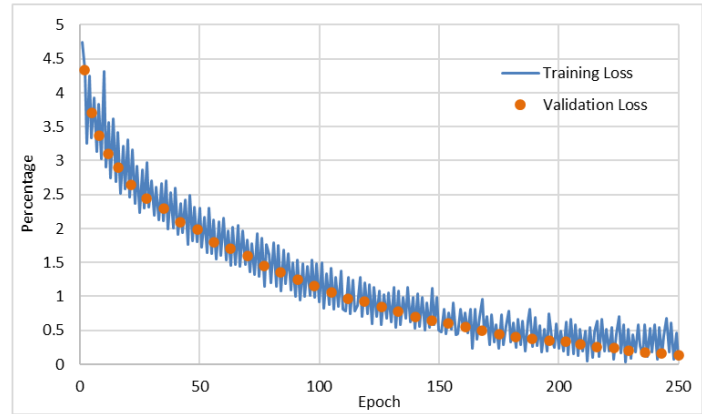
In Fig. 7, we present the confusion matrix created by the seven models on the dataset DT1. In the confusion matrix, T refers to data with brain tumors, and N refers to data from normal brains. The confusion matrix was built from the validation set of DT1 consisting of 600 data. It can be observed from the confusion matrix that the proposed model BrainTumorNet correctly predicts the most data and has the lowest incorrect predictions.

In Fig. 8(a), the progress of the performance accuracy of the proposed model (BrainTumorNet) on DT1 is illustrated. The performance of the model on 250 epochs is presented during both training and validation of the model. It can be observed that in the 1$^{st}$ epoch, the model starts with a very low training accuracy of 42% and validation accuracy of 54%. However, with each progressing epoch, the model's accuracy increases rapidly. On the final epoch, the model provides the highest training accuracy of 97.83% and validation accuracy of 98.66%.

Likewise, in Fig. 8(b), the progress of the loss of the proposed model (BrainTumorNet) over 250 epochs is presented. On the 1$^{st}$ epoch, the model demonstrates a high training loss of 4.75% and a validation loss of 4.33%. Over the increased epoch, the loss rate gradually decreases with consistency. On the final epoch, the model achieves the lowest training loss of 0.207% and validation loss of 0.135%.

## V.   STATE-OF-THE-ART COMPARISON

This paper introduces BrainTumorNet, a complex convolutional neural network (CNN) specifically designed for classifying images of brain tumors, to address the crucial difficulty of reliably identifying brain tumors using Magnetic Resonance Imaging (MRI). Advanced preparation techniques were used to ensure the highest level of data quality, including CLAHE for image improvement, data augmentation for assuring dataset variety, and blockchain integration for secure and traceable data administration. By recording accuracy scores of 98.66%, 97.17%, and 94.24% across three datasets during testing, BrainTumorNet demonstrated its outstanding abilities and established a new standard when compared to other pre-trained models. This study raises the standard for MRI-based brain tumor identification and gives professionals a crucial diagnostic tool. Table VI thoroughly evaluates BrainTumorNet's performance in relation to other existing models.

TABLE VI.    STATE-OF-THE-ART COMPARISON OF PROPOSED MODEL

| Authors | Data Type | Methods | Accuracy |
|---|---|---|---|
| Khan et al. [13] | MRI | Fine-tune VGG19 | 90.03% |
| Yahyaoui et al. [14] | MRI | DenseNet | 92.06% |
| Febrianto et al. [33] | MRI | CNN | 93% |
| Afshar et al. [34] | MRI | CapsNet | 90.89 |
| Anaraki et al. [35] | MRI | Shallow CNN | 94.20 |
| Rehman et al. [36] | MRI | 3D CNN | 92.67% |
| Sajjad et al. [37] | MRI | VGG19 | 90.67% |
| Banik et al. | MRI | BrainTumorNet | 98.66% |
| | | | 97.17% |
| | | | 94.24%. |

## VI.    CONCLUSION

BrainTumorNet, a CNN model developed to detect brain tumors from MRI images, was demonstrated in this research article. Its performance was improved through a rigorous data preparation process that included CLAHE and data augmentation. Brain TumorNet's unique incorporation of blockchain technology assures MRI data management that is highly secure and identifiable, thereby developing confidence and facilitating collaborations focused on data integrity. Assessed through the utilization of a wide variety of metrics such as accuracy, specificity, recall, precision, f1-score, and confusion matrix, BrainTumorNet demonstrated its ability to perform by attaining accuracy rates of 98.66%, 97.17%, and 94.24% on three separate datasets. Furthermore, it outperformed six pre-trained deep learning models. Despite infrequent misclassifications, its overall efficacy represents a significant development in the field of medical imaging. It is believed that integrating deep learning with blockchain will bring about an important change in perspective in healthcare management and brain tumor detection in the future.

### REFERENCES

[1] K. R. Bhatele and S. S. Bhadauria, ''Machine learning application in glioma classification: Review and comparison analysis,'' Arch. Comput. Methods Eng., vol. 29, pp. 247–274, Apr. 2021.

[2] M. Y. B. Murthy, A. Koteswararao, and M. S. Babu, ''Adaptive fuzzy deformable fusion and optimized CNN with ensemble classification for automated brain tumor diagnosis,'' Biomed. Eng. Lett., vol. 12, no. 1, pp. 37–58, Feb. 2022.

[3] R. Mehrotra, M. A. Ansari, R. Agrawal, and R. S. Anand, ''A transfer learning approach for AI-based classification of brain tumors,'' Mach. Learn. with Appl., vol. 2, Dec. 2020, Art. no. 100003.

[4] S. Grampurohit, V. Shalavadi, V. R. Dhotargavi, M. Kudari, and S. Jolad, ''Brain tumor detection using deep learning models,'' in Proc. IEEE India Council Int. Subsections Conf. (INDISCON), Oct. 2020, pp. 129–134.

[5] G. Raut, A. Raut, J. Bhagade, J. Bhagade, and S. Gavhane, ''Deep learning approach for brain tumor detection and segmentation,'' in Proc. Int. Conf. Converg. Digit. World Quo Vadis (ICCDW), Feb. 2020, pp. 1–5.

[6] T. C. Hollon, B. Pandian, A. R. Adapa, E. Urias, A. V. Save, S. S. S. Khalsa, D. G. Eichberg, R. S. D'Amico, Z. U. Farooq, S. Lewis, and P. D. Petridis, ''Near real-time intraoperative brain tumor diagnosis using stimulated Raman histology and deep neural networks,'' Nature Med., vol. 26, no. 1, pp. 52–58, Jan. 2020.

[7] Zhao, X., Wu, Y., Song, G., Li, Z., Zhang, Y., & Fan, Y. (2018). A deep learning model integrating FCNNs and CRFs for brain tumor segmentation. Medical image analysis, 43, 98-111.

[8] Mohsen, H., El-Dahshan, E. S. A., El-Horbaty, E. S. M., & Salem, A. B. M. (2018). Classification using deep learning neural networks for brain tumors. Future Computing and Informatics Journal, 3(1), 68-71.

[9] Paul, J. S., Plassard, A. J., Landman, B. A., & Fabbri, D. (2017, March). Deep learning for brain tumor classification. In Medical Imaging 2017: Biomedical Applications in Molecular, Structural, and Functional Imaging (Vol. 10137, pp. 253-268). SPIE.

[10] Ari, A., & Hanbay, D. (2018). Deep learning based brain tumor classification and detection system. Turkish Journal of Electrical Engineering and Computer Sciences, 26(5), 2275-2286.

[11] Abiwinanda, N., Hanif, M., Hesaputra, S. T., Handayani, A., & Mengko, T. R. (2019). Brain tumor classification using convolutional neural network. In World congress on medical physics and biomedical engineering 2018 (pp. 183-189). Springer, Singapore.

[12] Afshar, P., Plataniotis, K. N., & Mohammadi, A. (2019, May). Capsule networks for brain tumor classification based on MRI images and coarse tumor boundaries. In ICASSP 2019-2019 IEEE International Conference on Acoustics, Speech and Signal Processing (ICASSP) (pp. 1368-1372). IEEE.

[13] Khan, A. R., Khan, S., Harouni, M., Abbasi, R., Iqbal, S., & Mehmood, Z. (2021). Brain tumor segmentation using K - means clustering and deep learning with synthetic data augmentation for classification. Microscopy Research and Technique, 84(7), 1389-1399.

[14] Yahyaoui, H., Ghazouani, F., & Farah, I. R. (2021, July). Deep learning guided by an ontology for medical images classification using a multimodal fusion. In 2021 International Congress of Advanced Technology and Engineering (ICOTEN) (pp. 1-6). IEEE.

[15] Murthy, M. Y. B., Koteswararao, A., & Babu, M. S. (2022). Adaptive fuzzy deformable fusion and optimized CNN with ensemble classification for automated brain tumor diagnosis. Biomedical engineering letters, 12(1), 37-58.

[16] Latif, G., Ben Brahim, G., Iskandar, D. A., Bashar, A., & Alghazo, J. (2022). Glioma Tumors' classification using deep-neural-network-based features with SVM classifier. Diagnostics, 12(4), 1018.

[17] Kaggle. Avialble Online: https://www.kaggle.com/datasets/ ahmedhamada0/brain-tumor-detection?select=Br35H-Mask-RCNN (Accessed on 1 August 2023).

[18] Kaggle. Avialble Online: https://www.kaggle.com/datasets/ aryanfelix/brats-2019-traintestvalid?select=dataset (Accessed on 1 August 2023).

[19] Kaggle. Avialble Online: https://www.kaggle.com/datasets/mhantor/mri-based-brain-tumor-images (Accessed on 1 August 2023).

[20] Maymounkov P, Mazieres D. Kademlia: A peer-to-peer informa- ' tion system based on the XOR metric. In: Computer Science (Including Subseries Lecture Notes in Artificial Intelligence and Lecture Notes in Bioinformatics). (2002). doi: 10.1007/3-540-45748-8_5.

[21] Rahman A, Islam MJ, Montieri A, Nasir MK, Reza MM, Band SS, et al. SmartBlock-SDN: an optimized blockchain-SDN framework for resource management in IoT. IEEE Access. (2021) 9:28361–76. doi: 10.1109/ACCESS.2021.3058244.

[22] Krizhevsky, A.; Sutskever, I.; Hinton, G.E. Imagenet classification with deep convolutional neural networks. In Advances in Neural Information Processing Systems; Curran Associates, Inc.: New York, NY, USA, 2012; pp. 1097–1105.

[23] Pérez-Pérez, B. D., Garcia Vazquez, J. P., & Salomón-Torres, R. (2021). Evaluation of convolutional neural networks' hyperparameters with transfer learning to determine sorting of ripe medjool dates. Agriculture, 11(2), 115.

[24] He, K.; Zhang, X.; Ren, S.; Sun, J. Deep residual learning for image recognition. In Proceedings of the IEEE Conference on Computer Vision and Pattern Recognition, Las Vegas, NV, USA, 27–30 June 2016; pp. 770–778.

[25] Shamrat, F. J. M., Azam, S., Karim, A., Islam, R., Tasnim, Z., Ghosh, P., & De Boer, F. (2022). LungNet22: A Fine-Tuned Model for Multiclass Classification and Prediction of Lung Disease Using X-ray Images. Journal of personalized medicine, 12(5), 680.

[26] Zaccone, G.; Karim, M.R. Deep Learning with TensorFlow: Explore Neural Networks and Build Intelligent Systems with Python; Packt Publishing Ltd.: Birmingham, UK, 2018.

[27] Simonyan, K.; Zisserman, A. Very deep convolutional networks for large-scale image recognition. arXiv 2014, arXiv:1409.1556.

[28] Szegedy, C.; Vanhoucke, V.; Ioffe, S.; Shlens, J.; Wojna, Z. Rethinking the inception architecture for computer vision. In Proceedings of the IEEE Conference on Computer Vision and Pattern Recognition, Las Vegas, NV, USA, 27–30 June 2016; pp. 2818–2826.

[29] Huang, G., Liu, Z., Van Der Maaten, L., & Weinberger, K. Q. (2017). Densely connected convolutional networks. In Proceedings of the IEEE conference on computer vision and pattern recognition (pp. 4700-4708).

[30] Shamrat, F. J. M., Azam, S., Karim, A., Ahmed, K., Bui, F. M., & De Boer, F. (2023). High-precision multiclass classification of lung disease through customized MobileNetV2 from chest X-ray images. Computers in Biology and Medicine, 155, 106646.

[31] Shamrat, F. J. M., Akter, S., Azam, S., Karim, A., Ghosh, P., Tasnim, Z., & Ahmed, K. (2023). AlzheimerNet: An effective deep learning based proposition for alzheimer's disease stages classification from functional brain changes in magnetic resonance images. IEEE Access, 11, 16376-16395.

[32] Tasnim, Zarrin, et al. "Classification of breast cancer cell images using multiple convolution neural network architectures." International Journal of Advanced Computer Science and Applications 12.9 (2021).

[33] Febrianto, D. C., Soesanti, I., & Nugroho, H. A. (2020, March). Convolutional neural network for brain tumor detection. In IOP Conference Series: Materials Science and Engineering (Vol. 771, No. 1, p. 012031). IOP Publishing.

[34] Afshar, P., Plataniotis, K. N., & Mohammadi, A. (2019, May). Capsule networks for brain tumor classification based on MRI images and coarse tumor boundaries. In ICASSP 2019-2019 IEEE international conference on acoustics, speech and signal processing (ICASSP) (pp. 1368-1372). IEEE.

[35] Anaraki, A. K., Ayati, M., & Kazemi, F. (2019). Magnetic resonance imaging-based brain tumor grades classification and grading via convolutional neural networks and genetic algorithms. biocybernetics and biomedical engineering, 39(1), 63-74.

[36] Rehman, A., Khan, M. A., Saba, T., Mehmood, Z., Tariq, U., & Ayesha, N. (2021). Microscopic brain tumor detection and classification using 3D CNN and feature selection architecture. Microscopy Research and Technique, 84(1), 133-149.

[37] Sajjad, M., Khan, S., Muhammad, K., Wu, W., Ullah, A., & Baik, S. W. (2019). Multi-grade brain tumor classification using deep CNN with extensive data augmentation. Journal of computational science, 30, 174-182.

[38] Sandler, M., Howard, A., Zhu, M., Zhmoginov, A., & Chen, L. C. (2018). Mobilenetv2: Inverted residuals and linear bottlenecks. In Proceedings of the IEEE conference on computer vision and pattern recognition (pp. 4510-4520).